



Hemodynamic Parameters Predict In-stent Thrombosis After Multibranched Endovascular Repair of Complex Abdominal Aortic Aneurysms: A Retrospective Study of Branched Stent-Graft Thrombosis

OPEN ACCESS

Ming-Yuan Liu^{1,2†}, Yang Jiao^{3,4}, Junjun Liu⁵, Simeng Zhang^{6,7} and Wei Li^{3,4*}

Edited by:

Colin E. Evans,
Northwestern University, United States

Reviewed by:

Jiaxuan Feng,
Second Military Medical
University, China
Konstantinos Spanos,
University of Thessaly, Greece

*Correspondence:

Wei Li
mailto:wei@qq.com

†ORCID:

Ming-Yuan Liu
orcid.org/0000-0002-6449-4885

Specialty section:

This article was submitted to
Thrombosis,
a section of the journal
Frontiers in Cardiovascular Medicine

Received: 16 January 2021

Accepted: 22 March 2021

Published: 23 April 2021

Citation:

Liu M-Y, Jiao Y, Liu J, Zhang S and
Li W (2021) Hemodynamic
Parameters Predict In-stent
Thrombosis After Multibranched
Endovascular Repair of Complex
Abdominal Aortic Aneurysms: A
Retrospective Study of Branched
Stent-Graft Thrombosis.
Front. Cardiovasc. Med. 8:654412.
doi: 10.3389/fcvm.2021.654412

¹ Department of Vascular Surgery, Beijing Friendship Hospital, Capital Medical University, Beijing, China, ² Beijing Center for Vascular Surgery, Beijing, China, ³ Department of Vascular Surgery, Peking University People's Hospital, Beijing, China, ⁴ The Key Laboratory of Molecular Cardiovascular Science, Ministry of Education, Beijing, China, ⁵ Department of Vascular Surgery, The Affiliated Hospital of Qingdao University, Qingdao, China, ⁶ Department of Vascular Surgery, Changhai Hospital, Shanghai, China, ⁷ Department of Pediatric Cardiac Surgery, State Key Laboratory of Cardiovascular Disease, Fuwai Hospital, National Center for Cardiovascular Disease, Chinese Academy of Medical Sciences and Peking Union Medical College, Beijing, China

Background: Branch vessel occlusion is reported in endovascular repair of aortic pathology. This study aimed to evaluate the hemodynamic indicators associated with in-stent thrombosis (IST) of a branched stent-graft (BSG) after endovascular aortic repair (EVAR) of a complex abdominal aortic aneurysm.

Methods: A retrospective evaluation was performed based on the computed tomography (CT) scans and clinical data of three patients who underwent multi-branched endovascular repair. Patient-specific 3-dimensional models were reconstructed, and hemodynamic analysis was performed for IST. Hemodynamics-related parameters including time-averaged wall shear stress (TAWSS), oscillatory shear stress index (OSI), and relative residence time (RRT) were compared among the individual patients.

Results: The flow velocity, TAWSS, OSI, and RRT were radically changed in the area of the IST. In BSGs, IST tended to occur in the regions of hemodynamic alteration near the bends in the device, where a decreased flow velocity (<0.6 m/s) and TAWSS (<0.8 Pa) and an elevated OSI (>0.2) and RRT (>5 s) were consistently observed.

Conclusions: Hemodynamic perturbations in BSGs cause a predisposition to IST, which can be predicted by a series of changes in the flow parameters. Early hemodynamic analysis might be useful for identifying and remediating IST after multibranched endovascular repair.

Keywords: in-stent thrombosis, branched stent-grafts, computational fluid dynamic, endovascular aortic repair (EVAR), biomechanics

INTRODUCTION

The endovascular aortic repair (EVAR) has emerged as the “first choice” to treat abdominal aortic aneurysm (AAA) (1). For patients with thoracoabdominal or para-renal aneurysms that that not anatomically amenable to standard EVAR (2), a variety of approaches (3–5), including the physician modified stent grafts (PMSGs), the custom-made devices (CMDs) and the off the shelf devices, have been reported. However, the branched stent-graft (BSG) occlusion caused by the in-stent thrombosis (IST) has been reported in the clinical studies (6, 7), often leading to organ malperfusion (8). Morphological analysis alone might be insufficient to comprehensively evaluate the IST. Hemodynamics is considered to play a critical role in the formation and progression of IST (9, 10). Hemodynamic parameters might reveal the flow status of a BSG and provide quantifiable and even predictable evaluations of the IST, thus helping to inform medical decision making. However, the mechanism and hemodynamic characteristics of IST in BSG are poorly understood. Therefore, we aimed to evaluate the IST-related hemodynamic features of stent-grafts in this study.

METHODS

Patient Data

The CT images of three patients were imported into Mimics software (v19.0, Materialize, Ann Arbor, MI, USA) to build three-dimensional (3D) models. All CT scan images were obtained from Peking University People's Hospital (Beijing, China). Informed consent was obtained from all the patients, and the study protocols were approved by the Ethical Review Board and the Statistics Department of Peking University People's Hospital (No. 2017 PHB166-01). The pre- and postoperative CT scan images of three cases are shown in the upper and lower rows of **Figure 1A**, respectively. The mesh models of the three cases (based on the CT scan images) were all obtained at the 1 month follow-up and shown in **Figure 1B**. All three of these patients with complex AAAs were treated with physician-modified stent grafts (PMSGs) repair for the aorta (Endurant™, Medtronic, Santa Rosa, Calif, USA) and the visceral arteries (Viabahn™, W. L. Gore, Flagstaff, AZ, USA). The patients were administrated with anti-platelet (aspirin 100 mg/per day) and anticoagulants (Rivaroxaban 10 mg/per day) during the first month, and only administrated with anti-platelet (aspirin 100 mg/per day) thereafter. The procedural details are illustrated in **Figure 2**. The orientation of the proximal part of the branched stent grafts was modified based on the measurement of the preoperative CTA. The orientation of the cuff branches was preoperatively analyzed, and the stent-grafts

were deployed according to the preoperative measured angle and clock bit.

The celiac artery (CA), superior mesenteric artery (SMA), left renal artery (LRA), and right renal artery (RRA) were repaired in Case 1; the SMA and the bilateral renal arteries were repaired in both Case 2 and Case 3. In order to unify the models for comparison between different cases, the celiac artery in the Case 1 model was removed. In the case 2, the adopted model was the one with actual thrombosis developed in the BSG, which was confirmed by the CT scan (**Figure 3**). The models were smoothed and optimized in Geomagic Studio software (3D System, Morrisville, NC, USA) for the meshing process.

Mesh Generation and Computational Flow Dynamics (CFD) Simulations

Models were meshed using ICM software (ANSYS, Inc., Canonsburg, PA, USA). In order to achieve the same degree of accuracy for all simulations, the same maximum global base cell size of 2 mm was used for each model. A hybrid meshing method (11) comprising both tetrahedral and hexahedral elements was used in all models. In addition, prism layers were created near the boundaries to ensure the accuracy of the model meshing. The total number of elements in models of case 1–3 is 993470, 805931, and 785617, respectively. The meshes of three models are shown in **Figure 1B**. The mesh sensitive analysis did not reveal any significant difference of the vessels among 3 cases. Furthermore, the blood flow of the visceral arteries was not obviously altered between the cases. There was no significant association observed for pre and post-operative anatomy. The hemodynamic analysis did not recognize any anomaly alteration of hemodynamic parameters at the first month and 6 months among cases.

Boundary Conditions

The simulations were performed under pulsatile flow conditions, with the velocity profile (**Figure 1C**) as the inlet boundary conditions (12–15). *Outflow* conditions were used as outlet conditions, with the volume flow divided into 20.2% to the SMA, 19% to each renal artery, and 41.8% to the infrarenal aorta (16, 17). The flow ratio of each branch is marked in **Figure 1B**.

Assumptions and Governing Equations

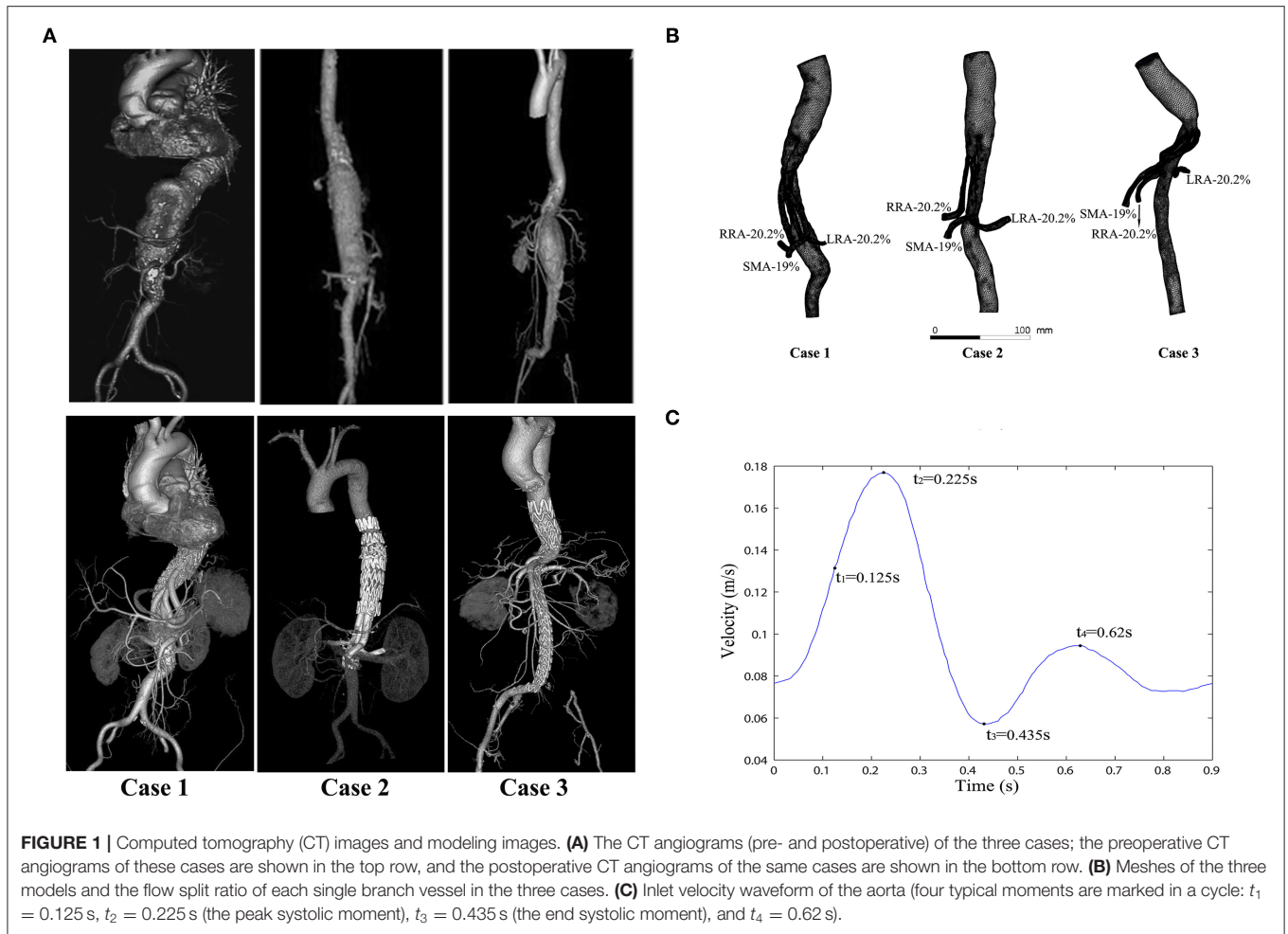
The blood was assumed to be an incompressible Newtonian fluid (18) with a dynamic viscosity of $0.0035 \text{ kg}\cdot\text{m}^{-1}\cdot\text{s}^{-1}$ and a density of $1,050 \text{ kg/m}^3$. The numerical simulation was based on the Navier-Stokes equation (neglecting gravity) and the conservation of mass:

$$\rho \left[\frac{\partial \vec{u}}{\partial t} + (\vec{u} \cdot \nabla) \vec{u} \right] + \nabla p - \mu \nabla^2 \vec{u} = 0 \quad (1)$$

$$\nabla \cdot \vec{u} = 0 \quad (2)$$

where \vec{u} and p , respectively, represent the fluid velocity vector and the pressure, while ρ and μ , respectively, are the density and viscosity of blood. The CFD software package ANSYS Fluent 14.5 (ANSYS, Lebanon, NH, USA) was used for the simulations.

Abbreviations: AAA, abdominal aortic aneurysm; EVAR, endovascular aortic repair; BSG, branched stent-graft; IST, in-stent thrombosis; CT, computed tomography; CA, celiac artery; SMA, superior mesenteric artery; LRA, left renal artery; RRA, right renal artery; TAWSS, time-averaged wall shear stress; OSI, oscillatory shear stress index; RRT, relative residence time; PMSGs, physician modified stent grafts; CMDs, custom made devices.



The pressure-based solver and SIMPLE algorithm were used for calculation.

The convergence criterion was set to 10^{-5} for both continuity and velocity residuals. A uniform time step of 0.005 s was chosen for all simulations. For each model, four cardiac cycles were carried out in each simulation process to obtain a periodic solution (19), and the results of the final cycle were used for post-processing and analysis (20).

Wall Shear Stress (WSS)-Related Parameters

This study focused particularly on the various near-wall hemodynamic (NWH) parameters that have been shown to have an effect on thrombus formation. Therefore, the time-averaged wall shear stress (TAWSS), used to describe the general features of WSS, in the pulsatile cycle was analyzed. The TAWSS was defined as follows:

$$TAWSS = \frac{1}{T} \int_0^T |WSS(s, t)| \cdot dt \quad (3)$$

where T is the duration of the cardiac cycle, WSS is the instantaneous wall shear stress vector, and s is the position on the vessel (or stent-graft) wall.

The oscillatory shear stress index (OSI) is a parameter that can describe the changing frequency of the WSS direction. It ranges from 0, where the flow is unidirectional and does not oscillate, to 0.5, where the WSS direction frequently changes.

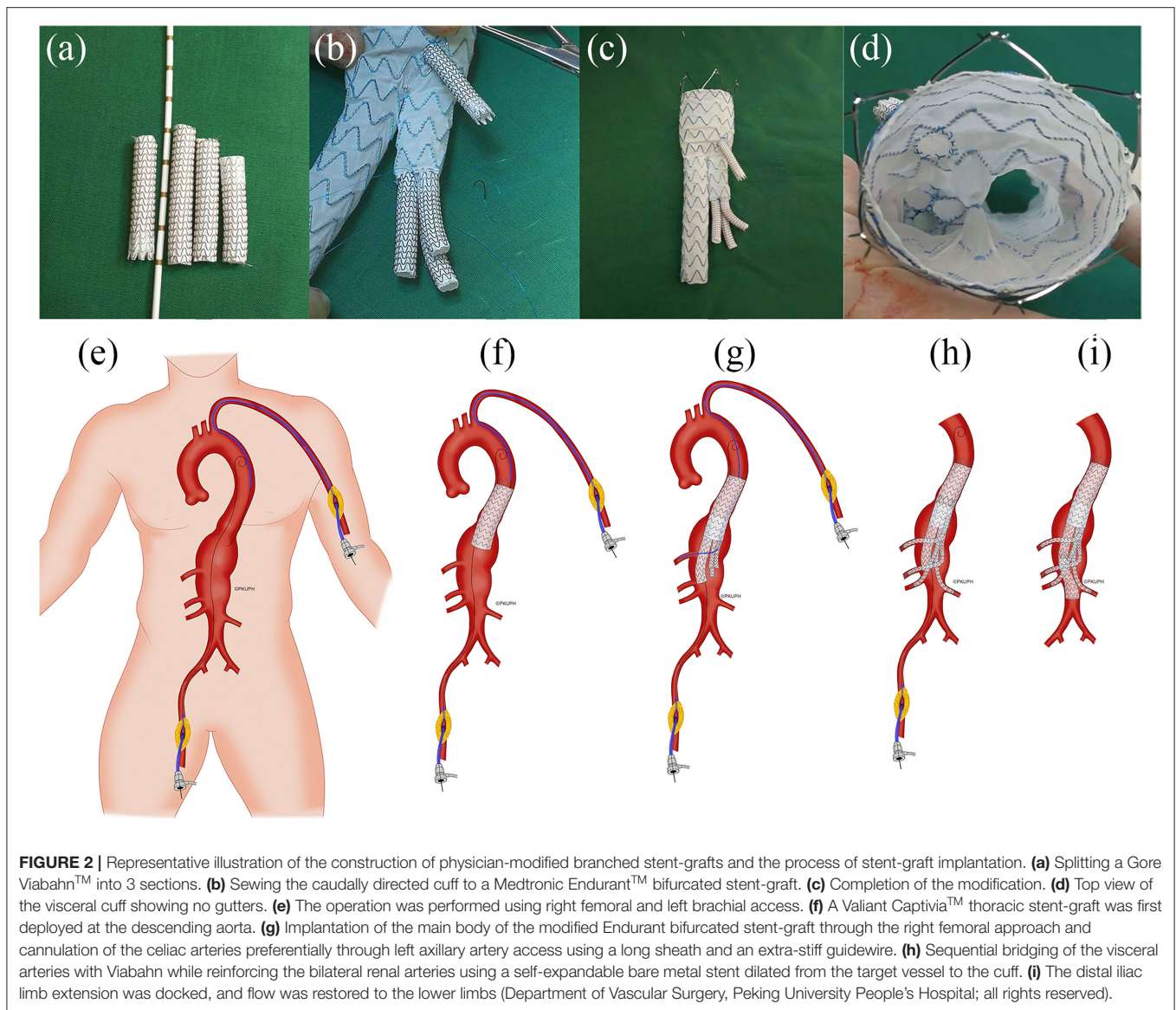
The OSI on the inner wall of the models was calculated as follows (21, 22).

$$OSI = 0.5 \left[1 - \left(\frac{|\frac{1}{T} \int_0^T WSS(s, t) \cdot dt|}{\frac{1}{T} \int_0^T |WSS(s, t)| \cdot dt} \right) \right] \quad (4)$$

where WSS is a vector parameter whose direction changes with the cardiac cycle time, T is the duration of the cardiac cycle, and s is the position on the vessel (or stent-graft) wall.

The relative residence time (RRT) is generally used to characterize the length of time that particles stay near the wall (23). This metric can reflect both OSI and TAWSS (24). The RRT is defined as:

$$RRT = \frac{1}{(1 - 2 \cdot OSI) \cdot TAWSS} \quad (5)$$



Data Analysis and Statistics

Qualitative and quantitative analyses of the full dataset were performed to observe local/global influences of the parameters of interest and their inter-correlation. Depending on the normality of the data, a 2-tailed t test or Mann-Whitney rank sum test was used to examine differences between continuous variables at the 4 time points (Replicated 3 times for each sections). The level of significance among the 4 hemodynamic parameters of interest (Velocity, TAWSS, OSI, RRT) were determined using one-way analysis of variance (ANOVA) followed by Dunnett's multiple comparisons test. Statistical analyses were performed using R (R Foundation for Statistical Computing, Vienna, Austria; <http://www.r-project.org>) and GraphPad Prism® version 7 (GraphPad, San Diego, CA); statistical significance was defined as $p < 0.05$.

RESULTS

Clinical Outcomes

Table 1 shows the demographic characteristics and clinical outcomes of the three patients. No complications were observed during the postoperative period in any of the three cases. During the follow-up period, Case 2 showed abdominal pain at 6 months after hospital discharge. CT angiography revealed that there was thrombosis in the BSG of the SMA and LRA (**Figure 3**). However, no IST was detected in either Case 1 or Case 3 (**Figure 3**).

Flow Velocity

Figure 4 shows the flow velocity in the three cases at four successive moments in the last cardiac cycle using four simulations ($t_1 = 0.125$ s, $t_2 = 0.225$ s, $t_3 = 0.435$ s, $t_4 = 0.62$ s). In order to reveal the flow characteristics of the BSG, the parameters are illustrated on the branched arterial region.

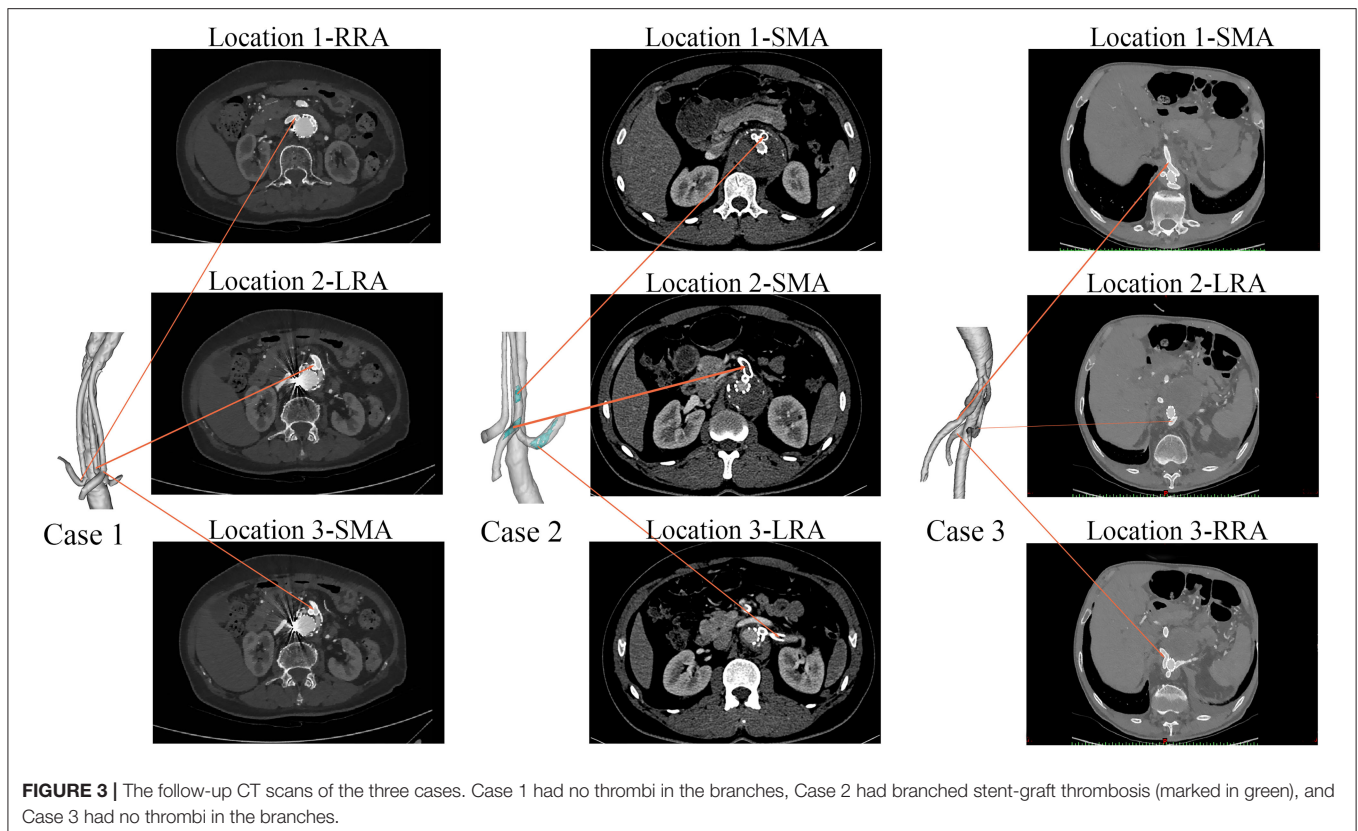


TABLE 1 | Demographic characteristics and clinical outcome of three cases.

	Case 1	Case 2	Case 3
Height (cm)	156	180	172
Weight (kg)	61	90	79
BMI	25.1	27.8	26.7
Gender	Female	Male	Male
Age	65	61	68
Follow-up time (months)	24	20	16
Blood pressure (mmHg)	130/91	120/81	150/90
BSG-IST	No	Yes	No
Velocity (m/s)	>0.6	<0.6	>0.6
TAWSS (Pa)	>0.8	<0.8	>0.8
OSI	<0.2	>0.2	<0.2
RRT (s)	<5	>5	<5
Stent-graft	Endurant™, 36-14-120 mm; 6*150 mm, Viabahn™	Endurant™, 38-14-120 mm; 6*150 mm, Viabahn™	Endurant™, 30-14-120 mm; 6*150 mm, Viabahn™

BMI, body mass index; BSG, branched stent-graft; IST, in-stent thrombosis; TAWSS, time-averaged wall shear stress; OSI, oscillatory shear stress index; RRT, relative residence time.

The streamlines for the three cases are shown in **Figures 4A–F**, and the magnitude of the velocity is indicated by the color. The locations of thrombosis in Case 2 were precisely matched with the identified low-velocity areas in **Figure 4C** where IST occurred in the BSGs. In order to investigate the velocity change in these low-velocity regions, cross-sections were taken from the

models of Case 1, Case 2, and Case 3. The velocity contours in different sections are also shown (**Figures 4B,D,F**). It was observed that the thrombosis/IST areas in Case 2, marked with black circles (**Figure 4C**), seemed to have lower velocity than the corresponding areas in Case 1 (**Figure 4A**) and Case 3 (**Figure 4E**) and lower velocity than the adjacent upstream and downstream areas in Case 2.

WSS, TAWSS, OSI, and RRT

Figure 5 shows the WSS distributions of the BSG through four successive moments in a cardiac cycle in each of the three cases. There was no remarkable change in the WSS along the BSG in Case 1 or Case 3. Nevertheless, low-WSS regions appeared over the course of the pulse cycle in Case 2, and the regions matched the IST area. Therefore, the hemodynamic parameters, including TAWSS, OSI and RRT, were analyzed to visualize the quantitative characteristics of the three cases. Contours of TAWSS, OSI and RRT on the walls of the stent-grafts are shown in **Figures 6A–C**. We found that the IST areas consistently matched the regions in which TAWSS, OSI and RRT were significantly altered in the BSGs. The IST area had a consistently lower values of velocity (<0.6 m/s) and TAWSS (<0.8 Pa), whereas a higher values of OSI (>0.2) and RRT (>5 s) than the non-thrombotic regions of the BSG.

DISCUSSION

Since PMSGs were introduced for the repair of complex aortic aneurysms (25), studies have amended the technique

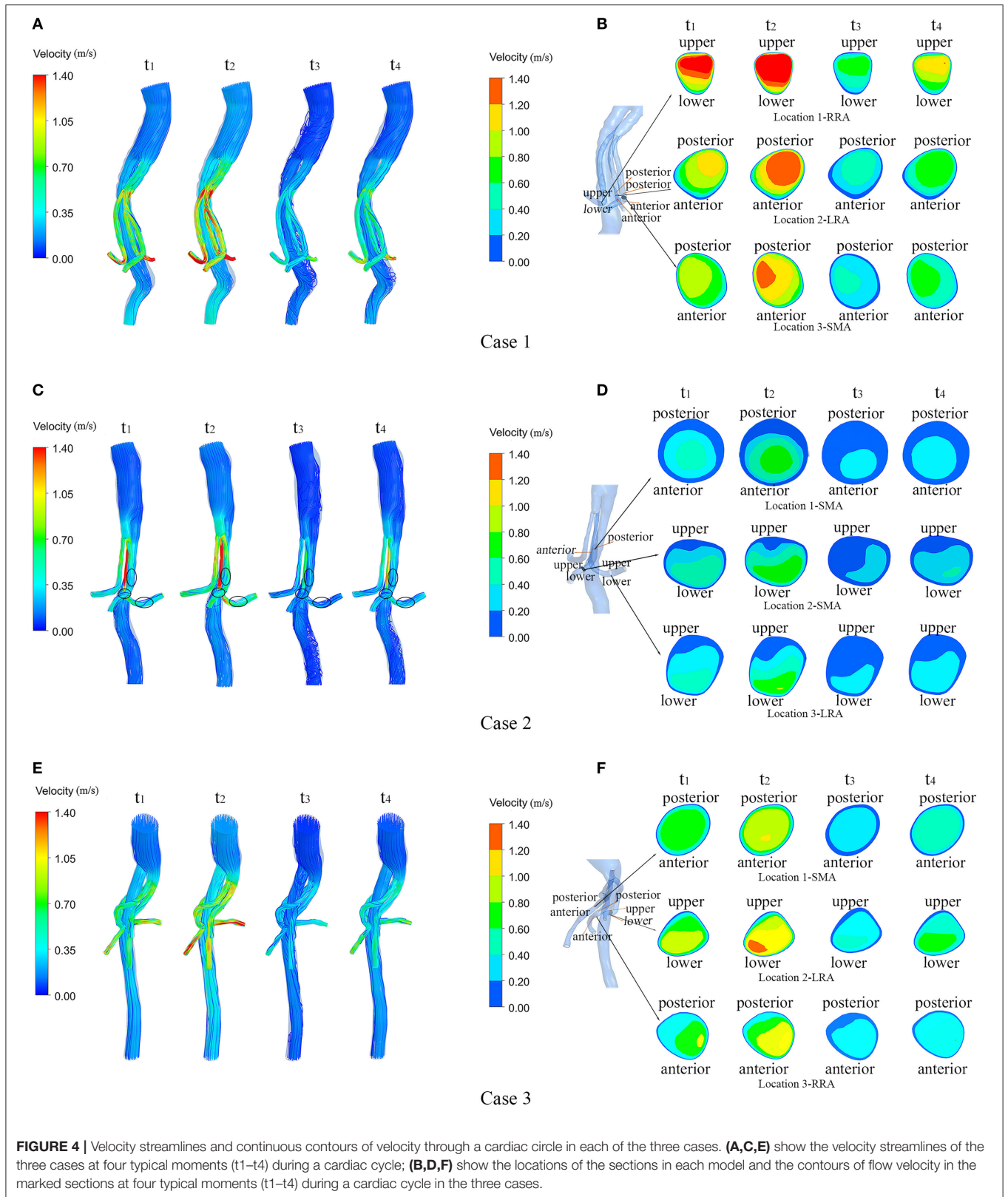


FIGURE 4 | Velocity streamlines and continuous contours of velocity through a cardiac circle in each of the three cases. **(A,C,E)** show the velocity streamlines of the three cases at four typical moments (t1–t4) during a cardiac cycle; **(B,D,F)** show the locations of the sections in each model and the contours of flow velocity in the marked sections at four typical moments (t1–t4) during a cardiac cycle in the three cases.

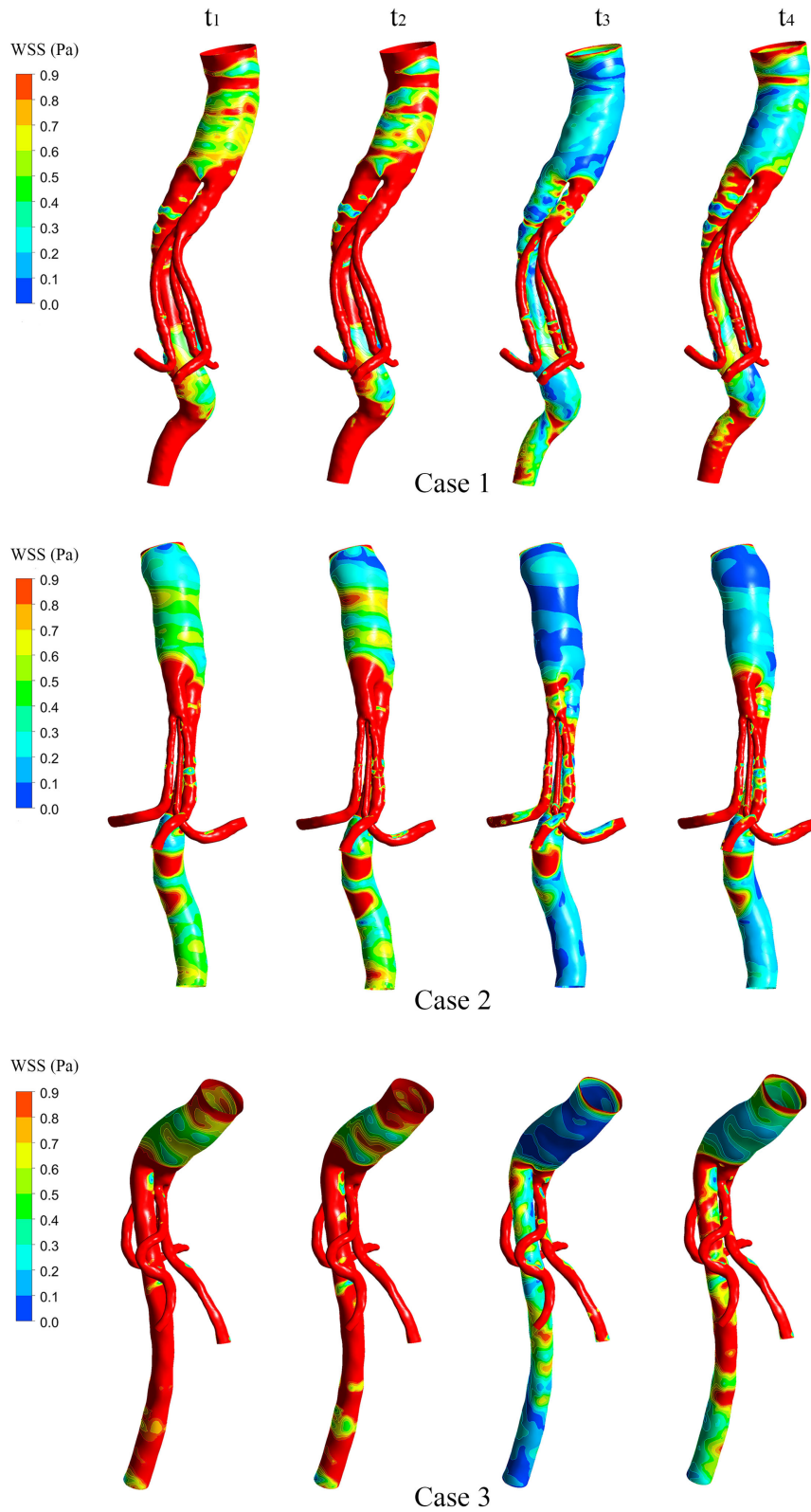


FIGURE 5 | The wall shear stress (WSS) distributions of the stent-grafts in three cases. The WSS is presented at the same four selected moments (t_1 - t_4) in each case.

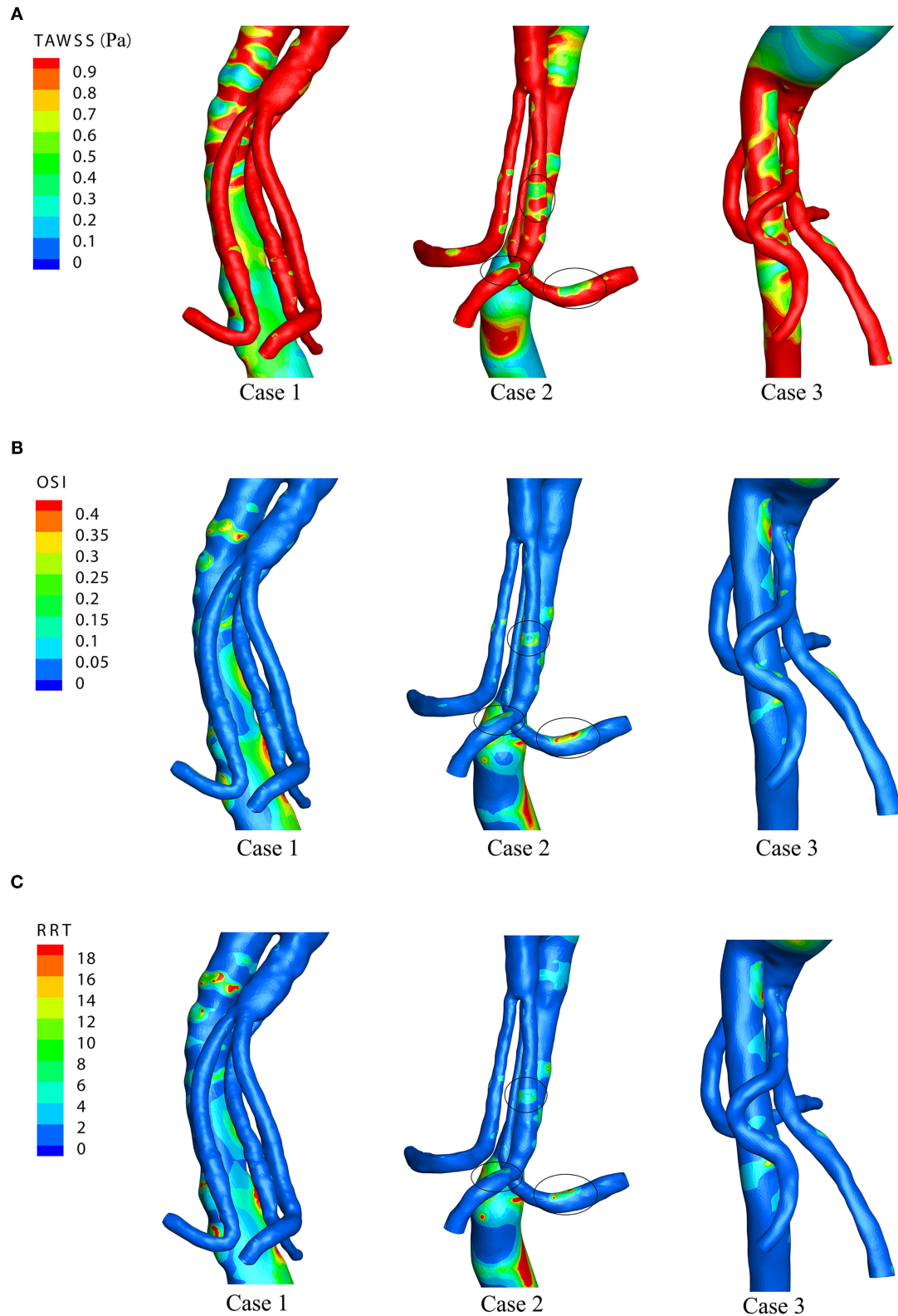


FIGURE 6 | The time-averaged wall shear stress (TAWSS), oscillatory shear index (OSI), and relative residence time (RRT) distributions of the three cases. **(A)** TAWSS distributions. **(B)** OSI distributions. **(C)** RRT distributions.

and demonstrated its feasibility and durability for patients with complex aortic aneurysms (26–28). Despite high technical success, however, visceral branch IST remains one of the leading complications after BSG implantation (29, 30). The flow characteristics of the BSG and the relationship between these characteristics and the IST remain largely unknown. Therefore, CFD with patient specific models were applied in this study to evaluate the hemodynamic mechanism of thrombosis within the visceral branches and explore IST-related hemodynamic parameters.

Low velocity is known to be associated with thrombosis. As shown in the velocity streamline diagram (Figure 4), the BSGs of Case 1 and Case 3 had higher velocities and more uniform flow patterns than the BSG of Case 2, and IST was observed in the marked areas (black circles). In Case 2, the velocity was significantly lower in the three marked (thrombosis) areas than in the upstream and downstream areas of the BSG (Figure 4) or in the corresponding locations of the other two cases.

Theoretically, low velocity induces a low TAWSS distribution (31). Our result demonstrated that the regions with low TAWSS (<0.8 Pa) (Figure 5) matched the regions with low flow velocity (<0.6 m/s) (Figure 4). Owing to the relevance of the WSS-related NWH hemodynamic parameters (Figure 6), we compared the TAWSS, OSI (an index to evaluate the fluctuation of the blood flow) and RRT and identified the consistent tendencies of these parameters. It has been reported that low WSS, high OSI and high RRT will promote platelet aggregation and ultimately lead to thrombus formation (31–33). Conti et al. showed that the femoro-popliteal in-stent thrombosis is characterized by larger diameter, low tortuosity, low flow velocity, low helicity, and low wall shear stress (34). Leg bending induces an overall increase of arterial tortuosity, helix flow, and reduces flow velocity which may furtherly promote the luminal area exposed to thrombosis related hemodynamic parameters. However, compared to the lower extremity, the stent-graft implanted in the visceral arteries were relatively steady to the lumbar vertebra, which may produce less helix flow rotation. Therefore, we used the established parameter-oscillatory shear index (19, 35) instead of helicity to address the turbulence in the endovascular aortic repair. In our results, the flow characteristics of TAWSS, OSI, and RRT were consistent in the non-thrombotic areas, whereas hemodynamic alteration appeared solely in the IST area. By analyzing the distribution of these parameters, we showed that the IST areas (Figure 3) matched the low-velocity areas (Figure 4). Furthermore, IST areas matched the areas of reduced TAWSS (Figure 6A), elevated OSI (Figure 6B), and RRT (Figure 6C). Our data have shown the hemodynamic parameters at the first month rather the 6 months. The configurations of the 3 patients with BSGs were not rigorously changed. The hemodynamic parameters were not statistically different at the first month and 6th months. The abnormal hemodynamics properties may not be observed at the very beginning. But it might be discovered and used to anticipate early thrombosis in a retrograde fashion. Together, these data demonstrated that hemodynamic perturbations introduced radical changes in hemodynamic parameters, which may predispose patients to IST. Alterations in hemodynamic parameters may be able to predict IST.

In a systematic review of off-the-shelf or physician-modified fenestrated and branched endografts, the author suggested that off-the-shelf and physician-modified technology seems effective and safe in both the elective and acute clinical outcome for the treatment of complex aortic aneurysms (29). The clinical outcomes of these techniques have been compared and reported in the articles (3, 36). Until for now, there is lack of literature that compared the hemodynamic differences under PMSGs, CMDs, or Off-the-shelf devices. With similarity in configurations, however, the hemodynamic environment underlying these modalities were unknown and it should be of great value to analyze the differences of hemodynamic characteristics. A variable flow properties characterized by flow separation, stagnation, low fluid velocity, and low WSS are associated with thrombosis and stenosis (10, 37). The curvature of the device and the change in diameter near the curved region can both contribute to these hemodynamic changes. In clinical practice, BSGs longer than the original vessels are almost invariably required for conveniently cannulation in the treatment of complex aortic aneurysms. Although a longer BSG would provide more gradual changes in momentum and allow blood flow to change gradually before reaching the target vessel (38), it would result in a curved portion, where the blood flow would be disturbed and thrombus-prone environments would be created. The hemodynamic parameters are known to be influenced by the highly curved and tortuous areas, which were commonly seen in the endovascular management for the complex aortic aneurysm. But what is not adequately described are, which certain types of hemodynamic changes (due to highly angled areas) were related to the in-stent thrombosis and whether these changes were of wide suitability among different techniques. In the present study, all three of the regions that developed IST after the procedure were at the bend of the BSG, which suggested that sharp curvature in a stent-graft adversely affects blood flow near the curved section, thereby accelerating thrombus formation. Therefore, we advocate preoperative planning to avoid sharp curvature at the bends of endografts.

Note that the PMSGs is a non-standardized technique and the long-term consequences of modifications remain unknown (39).

Research has illustrated the evolution from physician-modified to company-manufactured fenestrated-branched endografts in the treatment of complex and thoracoabdominal aortic aneurysms (36, 39). Through the evolution of devices, BSGs are typically used in multibranched endovascular aortic repairs. Despite the refinement of stent-grafts, preoperative design of the morphological configuration of the BSG should be considered. Our results suggested that sharp curvature in the BSG should be avoided and that early postoperative hemodynamic assessments of the BSG could assist in detecting predisposition toward IST after the operation. If the calculations identify regions with significantly changed hemodynamics in the BSG, special attention needs to be paid to these regions, as they may have an increased risk of IST. Our data indicated that relatively low velocity (<0.6 m/s) and TAWSS (<0.8 Pa) distributions and high OSI (>0.2) and RRT (>5 s) distributions were associated with the IST in the BSG. Therefore, high OSI and RRT and low TAWSS may predict the areas where IST will develop.

In contrast to the previous ideal model used to study branched stent configurations (16, 38), the models used in this study were derived from clinical cases, augmenting current knowledge with “real-world” data. Moreover, the models in this study provided important insights into the velocity and WSS distributions of BSGs.

LIMITATION

This study has several limitations that should be mentioned. First, only the fluid domain of the blood vessel was used for simulation. Although the interaction between stent-grafts and blood flow with the pulsatility of the flow were not considered in this study, the results are still reliable because it was a common practice in CFD analysis for fenestration endograft (40). Second, the stiffness and conformability of the bridging stents are important and it should be addressed by rigorous mechanics analysis. However, this condition cannot be achieved at present. Third, it should be noticed that the PMSGs was used outside the instruction for use and it should be used in the condition when validated treatments are not available. PMSGs is a non-standardized technique and the long-term consequences of modifications remain unknown. Although the patient specific models may improve computational simulation and integrate further details, the sample size was limited in our study. We recommend further evaluation with a large sample size, patient-specific boundaries, and long-term follow-up to validate these findings.

CONCLUSION

This study found that anomaly hemodynamic parameters predispose patients to IST within BSGs. Analysis of these parameters in the early postoperative period may be beneficial for identifying and remediating IST after multibranched endovascular aortic repair.

DATA AVAILABILITY STATEMENT

The data that support the findings of this study are available from Peking University People’s Hospital, but restrictions apply to the availability of these data, which were used under license for the current study and therefore are not publicly available. The

REFERENCES

1. Debono S, Nash J, Tambyraja AL, Newby DE, Forsythe OR. Endovascular repair for abdominal aortic aneurysms. *Heart*. (2021). doi: 10.1136/heartjnl-2020-318288. [Epub ahead of print].
2. Marzelle J, Presles E, Becquemin JP. Results and factors affecting early outcome of fenestrated and/or branched stent grafts for aortic aneurysms: a multicenter prospective study. *Ann Surg*. (2015) 261:197–206. doi: 10.1097/SLA.0000000000000612
3. Oderich GS, Ribeiro MS, Sandri GA, Tenorio ER, Hofer JM, Mendes BC, et al. Evolution from physician-modified to company-manufactured fenestrated-branched endografts to treat pararenal and thoracoabdominal aortic aneurysms. *J Vasc Surg*. (2019) 70:31–42.e7. doi: 10.1016/j.jvs.2018.09.063

data are, however, available from the authors upon reasonable request and with permission of the Ethical Review Board, Peking University People’s Hospital.

ETHICS STATEMENT

The authors confirmed that all experimental protocols involving human data in this study were in compliance with national/international/institutional guidelines or the Declaration of Helsinki. Informed consent was obtained from all the patients, and the study protocols were approved by the Ethical Review Board and Statistics Department of Peking University People’s Hospital (No. 2017 PHB166-01). Consent for publication was obtained from all participants.

AUTHOR CONTRIBUTIONS

M-YL and WL were contributed to the conception and study design, obtaining funding, writing the article, and critical revision of the article. YJ and JL were contributed to the data collection, analysis, and interpretation. SZ was contributed to the obtaining funding.

FUNDING

This work was supported by the National Natural Science Foundation of China (NSFC, Nos. 81470574, 82000429, and 81800403), Peking University Medicine Seed Fund for Interdisciplinary Research supported by the Fundamental Research Funds for the Central Universities, Beijing Municipal Hospital Scientific Research Training Program Foundation (PX2021002), and Scientific and Technology Program of Beijing Education Commission (KM202110025016).

ACKNOWLEDGMENTS

The authors appreciated Drs. Anqiang Sun, Xiaoyan Deng, and Yunqing Mu for their assistance with hemodynamic analysis. The authors also thanked the help from the Statistical Department of Peking University People’s Hospital.

4. Farber MA, Oderich GS, Timaran C, Sanchez LA, Dawson ZI, Zenith p-Branch Feasibility Study. Results from a prospective multicenter feasibility study of Zenith p-Branch stent graft. *J Vasc Surg*. (2019) 70:1409–18.e3 doi: 10.1016/j.jvs.2019.03.026
5. Cochenec F, Kobeiter H, Gohel M, Leopardi M, Raux M, Majewski M, et al. Early results of physician modified fenestrated stent grafts for the treatment of thoraco-abdominal aortic aneurysms. *Eur J Vasc Endovasc Surg*. (2015) 50:583–92 doi: 10.1016/j.ejvs.2015.07.002
6. Polaczyk A, Podyma M, Stefanczyk L, Szubert W, Zbicinski I. A 3D model of thrombus formation in a stent-graft after implantation in the abdominal aorta. *J Biomech*. (2015) 48:425–31. doi: 10.1016/j.jbiomech.2014.12.033

7. Starnes BW. Physician-modified endovascular grafts for the treatment of elective, symptomatic, or ruptured juxtarenal aortic aneurysms. *J Vasc Surg.* (2012) 56:601–7. doi: 10.1016/j.jvs.2012.02.011
8. Ou J, Chan YC W, Cheng S. A systematic review of fenestrated endovascular repair for juxtarenal and short-neck aortic aneurysm: evidence so far. *Ann Vasc Surg.* (2015) 29:1680–8. doi: 10.1016/j.avsg.2015.06.074
9. Rayz VL, Boussel L, Ge L, Leach JR, Martin AJ, Lawton MT, et al. Saloner: flow residence time and regions of intraluminal thrombus deposition in intracranial aneurysms. *Ann Biomed Eng.* (2010) 38:3058–69. doi: 10.1007/s10439-010-0065-8
10. Wootton DM, Ku ND. Fluid mechanics of vascular systems, diseases, and thrombosis. *Annu Rev Biomed Eng.* (1999) 1:299–329. doi: 10.1146/annurev.bioeng.1.1.299
11. Chiastra C, Morlacchi S, Pereira S, Dubini G, Migliavacca F. Computational fluid dynamics of stented coronary bifurcations studied with a hybrid discretization method. *Eur J Mech B/Fluids.* (2012) 35:76–84. doi: 10.1016/j.euromechflu.2012.01.011
12. Rogers IS, Massaro JM, Truong QA, Mahabadi AA, Kriegel MF, Fox CS, et al. Distribution, determinants, and normal reference values of thoracic and abdominal aortic diameters by computed tomography (from the Framingham Heart Study). *Am J Cardiol.* (2013) 111:1510–6. doi: 10.1016/j.amjcard.2013.01.306
13. Taylor CA, Hughes TJ, Zarins KC. Finite element modeling of three-dimensional pulsatile flow in the abdominal aorta: relevance to atherosclerosis. *Ann Biomed Eng.* (1998) 26:975–87. doi: 10.1114/1.140
14. Moore JE, Ku DN. Pulsatile velocity measurements in a model of the human abdominal aorta under resting conditions. *J Biomech Eng.* (1994) 116:337–46. doi: 10.1115/1.2895740
15. Aronberg DJ, Glazer HS, Madsen K, Sagel SS. Normal thoracic aortic diameters by computed tomography. *J Comput Assist Tomogr.* (1984) 8:247–50.
16. Suess T, Anderson J, Sherman A, Remund T, Pohlson K, Mani G, et al. Shear accumulation as a means for evaluating risk of thromboembolic events in novel endovascular stent graft designs. *J Vasc Surg.* (2017) 65:1813–9. doi: 10.1016/j.jvs.2016.07.108
17. Ku DN, Glagov S, Moore JE, Zarins CK. Flow patterns in the abdominal aorta under simulated postprandial and exercise conditions: an experimental study. *J Vasc Surg.* (1989) 9:309–16. doi: 10.1016/0741-5214(89)90051-7
18. Wang Z, Sun A, Fan Y, Deng X. Comparative study of Newtonian and non-Newtonian simulations of drug transport in a model drug-eluting stent. *Biorheology.* (2012) 49:249–59. doi: 10.3233/BIR-2012-0607
19. Kandail H, Hamady M, Xu YX. Patient-specific analysis of displacement forces acting on fenestrated stent grafts for endovascular aneurysm repair. *J Biomech.* (2014) 47:3546–54. doi: 10.1016/j.jbiomech.2014.08.011
20. Massai D, Soloperto G, Gallo D, Xu X, Morbiducci U. Shear-induced platelet activation and its relationship with blood flow topology in a numerical model of stenosed carotid bifurcation. *Eur J Mech B-Fluids.* (2012) 35:92–101. doi: 10.1016/j.euromechflu.2012.03.011
21. Del Alamo JC, Meili R, Alonso-Latorre B, Rodriguez-Rodriguez J, Aliseda A, Firtel RA, et al. Spatio-temporal analysis of eukaryotic cell motility by improved force cytometry. *Proc Natl Acad Sci USA.* (2007) 104:13343–8. doi: 10.1073/pnas.0705815104
22. He X, Ku ND. Pulsatile flow in the human left coronary artery bifurcation: average conditions. *J Biomech Eng.* (1996) 118:74–82. doi: 10.1115/1.2795948
23. Himburg HA, Grzybowski DM, Hazel AL, LaMack JA, Li XM, Friedman HM. Spatial comparison between wall shear stress measures and porcine arterial endothelial permeability. *Am J Physiol Heart Circ Physiol.* (2004) 286:H1916–22. doi: 10.1152/ajpheart.00897.2003
24. Lee SW, Antiga L, Steinman AD. Correlations among indicators of disturbed flow at the normal carotid bifurcation. *J Biomech Eng.* (2009) 131:061013. doi: 10.1115/1.3127252
25. Anderson J, Nykamp M, Danielson L, Remund T, Kelly WP. A novel endovascular debranching technique using physician-assembled endografts for repair of thoracoabdominal aneurysms. *J Vasc Surg.* (2014) 60:1177–84. doi: 10.1016/j.jvs.2014.05.090
26. Motta F, Crowner JR, Kalbaugh CA, Marston WA, Pascarella L, McGinagle KL, et al. Outcomes and complications after fenestrated-branched endovascular aortic repair. *J Vasc Surg.* (2019) 70:15–22. doi: 10.1016/j.jvs.2018.10.052
27. Oderich GS, Ribeiro M, Hofer J, Wigham J, Cha S, Chini J, et al. Prospective, nonrandomized study to evaluate endovascular repair of pararenal and thoracoabdominal aortic aneurysms using fenestrated-branched endografts based on supraceliac sealing zones. *J Vasc Surg.* (2017) 65:1249–59.e10. doi: 10.1016/j.jvs.2016.09.038
28. Verhoeven EL, Katsargyris A, Bekkema F, Oikonomou K, Zeebregts CJ, Ritter W, et al. Editor's choice - ten-year experience with endovascular repair of thoracoabdominal aortic aneurysms: results from 166 consecutive patients. *Eur J Vasc Endovasc Surg.* (2015) 49:524–31. doi: 10.1016/j.ejvs.2014.11.018
29. Georgiadis GS, van Herwaarden JA, Antoniou GA, Hazenberg CE, Giannoukas AD, Lazarides MK, et al. Systematic review of off-the-shelf or physician-modified fenestrated and branched endografts. *J Endovasc Ther.* (2016) 23:98–109. doi: 10.1177/1526602815611887
30. Premprabha D, Sobel J, Pua C, Chong K, Reilly LM, Chuter TA, et al. Visceral branch occlusion following aneurysm repair using multibranch thoracoabdominal stent-grafts. *J Endovasc Ther.* (2014) 21:783–90. doi: 10.1583/14-4807R.1
31. Xue Y, Liu X, Sun A, Zhang P, Fan Y, Deng X. Hemodynamic performance of a new punched stent strut: a numerical study. *Artif Organs.* (2016) 40:669–77. doi: 10.1111/aor.12638
32. Taylor JO, Meyer RS, Deutsch S, Manning BK. Development of a computational model for macroscopic predictions of device-induced thrombosis. *Biomech Model Mechanobiol.* (2016) 15:1713–31. doi: 10.1007/s10237-016-0793-2
33. Kolandaivelu K, Swaminathan R, Gibson WJ, Kolachalama VB, Nguyen-Ehrenreich KL, Giddings VL, et al. Stent thrombogenicity early in high-risk interventional settings is driven by stent design and deployment and protected by polymer-drug coatings. *Circulation.* (2011) 123:1400–9. doi: 10.1161/CIRCULATIONAHA.110.003210
34. Conti M, Ferrarini A, Finotello A, Salsano G, Auricchio F, Palombo D, et al. Patient-specific computational fluid dynamics of femoropopliteal stent-graft thrombosis. *Med Eng Phys.* (2020) 86:57–64. doi: 10.1016/j.medengphy.2020.10.011
35. Tricarico R, Tran-Son-Tay R, Laquian L, Scali ST, Lee TC, Beck AW, et al. Haemodynamics of different configurations of a left subclavian artery stent graft for thoracic endovascular aortic repair. *Eur J Vasc Endovasc Surg.* (2020) 59:7–15. doi: 10.1016/j.ejvs.2019.06.028
36. Chuter TA, Hiramoto JS, Park KH, Reilly ML. The transition from custom-made to standardized multibranch thoracoabdominal aortic stent grafts. *J Vasc Surg.* (2011) 54:660–7; discussion 667–8. doi: 10.1016/j.jvs.2011.03.005
37. Sun A, Fan Y, Deng X. Numerical comparative study on the hemodynamic performance of a new helical graft with noncircular cross section and SwirlGraft. *Artif Organs.* (2010) 34:22–7. doi: 10.1111/j.1525-1594.2009.00797.x
38. Suess T, Anderson J, Danielson L, Pohlson K, Remund T, Blears E, et al. Examination of near-wall hemodynamic parameters in the renal bridging stent of various stent configurations for repairing visceral branched aortic aneurysms. *J Vasc Surg.* (2016) 64:788–96. doi: 10.1016/j.jvs.2015.04.421
39. Canonge J, Jayet J, Heim F, Chakfe N, Coggia M, Coscas RF. Comprehensive review of physician modified aortic stent grafts: technical and clinical outcomes. *Eur J Vasc Endovasc Surg.* (2021) 9;S1530-891X(21)00042-2. doi: 10.1016/j.ejvs.2021.01.019
40. Avrahami I, Brand M, Meirson T, Ovadia-Blechman Z, Halak M. Hemodynamic and mechanical aspects of fenestrated endografts for treatment of abdominal aortic aneurysm. *Eur J Mech B/Fluids.* (2012) 35:85–91. doi: 10.1016/j.euromechflu.2012.03.010

Conflict of Interest: The authors declare that the research was conducted in the absence of any commercial or financial relationships that could be construed as a potential conflict of interest.

Copyright © 2021 Liu, Jiao, Liu, Zhang and Li. This is an open-access article distributed under the terms of the Creative Commons Attribution License (CC BY). The use, distribution or reproduction in other forums is permitted, provided the original author(s) and the copyright owner(s) are credited and that the original publication in this journal is cited, in accordance with accepted academic practice. No use, distribution or reproduction is permitted which does not comply with these terms.